

## Simulation and numerical study of two-phase flow in a centrifugal dust catcher

F Kh Nazarov<sup>1</sup>, Z M Malikov<sup>1</sup>, N M Rakhmanov<sup>2</sup>

<sup>1</sup>Institute of Mechanics and Seismic Stability of Structures of the Academy of Sciences of the Republic of Uzbekistan

<sup>2</sup>Tashkent State Technical University, 100125, Tashkent, Republic of Uzbekistan,

malikov.z62@mail.ru, farruxnazar@mail.ru, nizomiddinr@gmail.com

**Abstract.** Numerical study of turbulent swirling air flow with solid particles in a centrifugal dust catcher is carried out in this paper. The Spalart-Allmaras modified turbulence model (SARC) has been used to construct a mathematical model with account of the interaction between solid particles and air mass. The Lagrange approach has been used to study the trajectory of solid particles. The numerical results obtained are compared with experimental data. The experiment has been conducted with zinc powder on a laboratory stand of a centrifugal dust catcher. ...

Multiphase turbulent swirling flows are widely used to intensify the processes of heat and mass transfer in various industrial devices, such as chemical reactors, combustion chambers, dust catchers, separators, etc.

In this paper, the two-phase turbulent flow is studied in a centrifugal dust catcher (a cyclone).

Fig. 1 shows a schematic diagram of a laboratory centrifugal dust catcher. As seen from the figure, the dust catcher contains a cylindrical part and a conical part.

The principle of operation of this device lies in the fact that at the end of the discharge pipe 3-3 air suction creates a vacuum zone. As a result of this, a dust-air flow enters the inlet 1 of the dust catcher; passing through the tangential swirler, it swirls. The swirling flow leaving the swirler enters the coaxial space 1-1 of cross section  $\xi = 0$ .

Beginning from  $\xi = 0$ , dust particles due to centrifugal force are shifted to the outer wall. In the cross section  $\xi = 0.2$ , the conical part of the dust catcher begins; here the dust particles along the inner wall of the cone are directed downwards and in the cross section  $\xi = 1$  fall into a vacuum-sealed bunker. The air is directed to the discharge pipe, i.e. to 3-3 zone. To study experimentally the characteristics of the dust catcher, the dust is fed into the inlet of the dust catcher, then, the dust is entrained by the air inside the device. In the laboratory stand, the air after the discharge pipe enters the bag filter, where the dust not settled in the centrifugal dust catcher is collected.

In practice, the volume density of dust in dust catchers can reach  $50 \text{ g/m}^3$ . This value is significantly less than the density of incompressible air ( $2.5 \text{ kg/m}^3$ ). Therefore, the effect of the solid phase on the dynamics of air is often neglected. However, near the wall, where the dust particles accumulate under centrifugal force, the density of the solid phase can reach significant values. In these cases, the effect of the solid phase on the dynamics of the gas phase cannot be neglected. So, in this



paper, a numerical study of the turbulent flow is carried out taking into account the effect of the solid phase on the air flow inside the centrifugal unit.

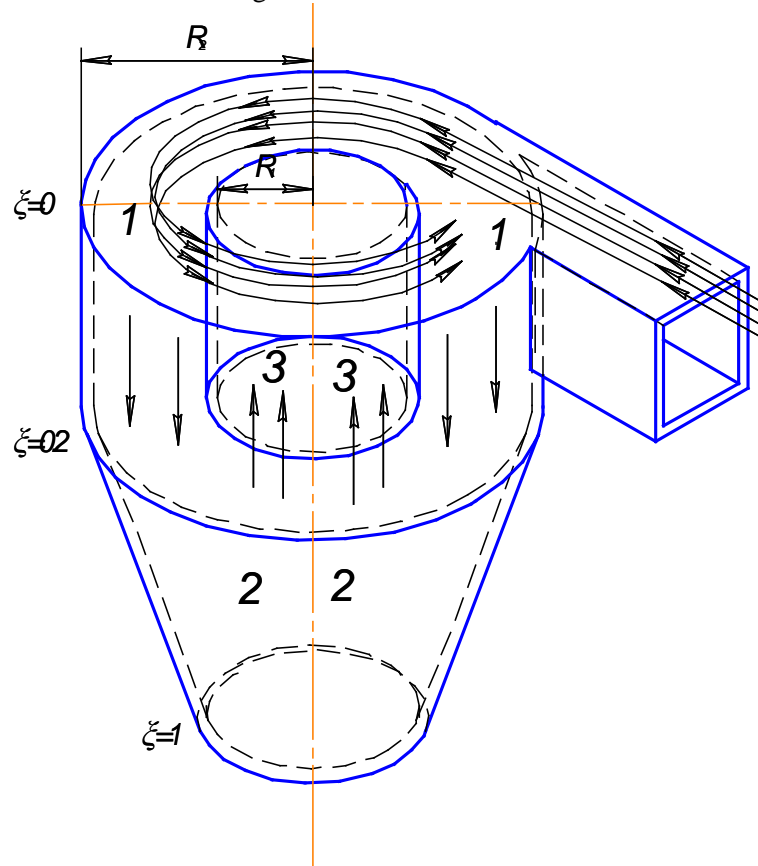


**Figure 1.** Schematic diagram of a centrifugal dust collector

It is known that swirling flows are characterized by a strong flow curvature, the occurrence of recirculation zones, the location and size of which largely depend on the intensity of the swirl and configuration of the boundaries. Since such flows are turbulent, more exact models of turbulence are required for their study.

Recently, quite effective turbulence models have appeared [1–2], which have been modified to apply to turbulent flows with a swirl [3–4]. The SARC turbulence model [3] is used in the paper to describe the turbulent viscosity  $\nu_t$ .

There is no single concept on modeling the kinematics of particle motion in a turbulent two-phase flow which would allow correct describing of the object [5]. The model based on the concept of “trajectory particles” is considered incorrect due to the lack of consideration for the factor of Reynolds stresses and particles interaction. On the other hand, the advantages of the Lagrange approach, which is closer to real processes and allows obtaining the necessary information about the trajectories of particles, the residence time of particles in the device, the minimum size of particles to be caught, are undeniable [6–9]. In this connection, in the present study, the Lagrange approach is used to model the efficiency of the centrifugal dust catcher.

The system of equations for a nonstationary incompressible axisymmetric turbulent gas flow with solid inclusions in a cylindrical coordinate system with the  $z$  axis along the channel axis and the radial coordinate  $r$  is written as [10]:

In this system  $V_z, V_r, V_\varphi$  are the axial, radial and tangential components of the airflow velocity vector, respectively;  $\vartheta_{iz}, \vartheta_{ir}, \vartheta_{i\varphi}$  are the similar components of the velocity vector for the  $i$ -th dust fraction;  $p$  is the pressure;  $\rho$  is the gas density;  $\nu$  is its molecular viscosity;  $\nu_t$  is the turbulent viscosity

of the air flow;  $\rho_i$  is the mass density of dust;  $k_i$  is the coefficient of interaction between air and the  $i$ -th fraction of dust;  $D$  is the diffusion coefficient of the solid phase,  $Sc = 0.8$  is the Schmidt coefficient.

$$\left\{ \begin{aligned} & \frac{\partial V_z}{\partial z} + \frac{\partial r V_r}{r \partial r} = 0, \\ & \frac{\partial V_z}{\partial t} + V_r \frac{\partial V_z}{\partial r} + V_z \frac{\partial V_z}{\partial z} + \frac{1}{\rho} \frac{\partial P}{\partial z} = \frac{1}{r} \frac{\partial}{\partial r} \left[ r \tilde{v} \frac{\partial V_z}{\partial r} \right] - \sum_{i=1}^N \frac{\rho_i}{\rho} k_i (V_z - \mathcal{G}_{iz}), \\ & \frac{\partial V_r}{\partial t} + V_r \frac{\partial V_r}{\partial r} + V_z \frac{\partial V_r}{\partial z} - \frac{v_\varphi^2}{r} + \frac{1}{\rho} \frac{\partial P}{\partial r} = \frac{1}{r} \frac{\partial}{\partial r} \left[ r \tilde{v} \frac{\partial V_r}{\partial r} \right] - \sum_{i=1}^N \frac{\rho_i}{\rho} k_i (V_r - \mathcal{G}_{ir}), \\ & \frac{\partial V_\varphi}{\partial t} + V_r \frac{\partial V_\varphi}{\partial r} + V_z \frac{\partial V_\varphi}{\partial z} + \frac{\mathcal{G}_\varphi \mathcal{G}_r}{r} = \frac{1}{r} \frac{\partial}{\partial r} \left[ r \tilde{v} \frac{\partial V_\varphi}{\partial r} \right] - \frac{\tilde{v}}{r^2} V_\varphi - \sum_{i=1}^N \frac{\rho_i}{\rho} k_i (V_\varphi - \mathcal{G}_{i\varphi}), \\ & \frac{\partial \rho_i}{\partial t} + \frac{\partial r \rho_i \mathcal{G}_{ir}}{r \partial r} + \frac{\partial \rho_i \mathcal{G}_{iz}}{\partial z} = 0, \\ & \frac{\partial \mathcal{G}_{iz}}{\partial t} + \mathcal{G}_{ir} \frac{\partial \mathcal{G}_{iz}}{\partial r} + \mathcal{G}_{iz} \frac{\partial \mathcal{G}_{iz}}{\partial z} = k_i (V_z - \mathcal{G}_{iz}), \\ & \frac{\partial \mathcal{G}_{ir}}{\partial t} + \mathcal{G}_{ir} \frac{\partial \mathcal{G}_{ir}}{\partial r} + \mathcal{G}_{iz} \frac{\partial \mathcal{G}_{ir}}{\partial z} - \frac{v_{i\varphi}^2}{r} = k_i (V_r - \mathcal{G}_{ir}), \\ & \frac{\partial \mathcal{G}_{i\varphi}}{\partial t} + \mathcal{G}_{ir} \frac{\partial \mathcal{G}_{i\varphi}}{\partial r} + \mathcal{G}_{iz} \frac{\partial \mathcal{G}_{i\varphi}}{\partial z} + \frac{\mathcal{G}_{i\varphi} \mathcal{G}_{ir}}{r} = k_i (V_\varphi - \mathcal{G}_{i\varphi}), \\ & D = \frac{\rho}{\rho + \rho_p} \frac{v + v_t}{Sc}, \\ & \tilde{v} = v + v_t. \end{aligned} \right. \tag{1}$$

The interaction coefficient between the phases is defined as the Stokes parameter:

$$k_i = \frac{18\rho v}{\rho^0 \delta_i^2}. \tag{2}$$

In this expression,  $\rho^0$  is the density of material of dust particles,  $\delta_i$  is the “effective” diameter of the particles.

As mentioned above for the calculation of particle paths, the Lagrange approach is convenient. For this purpose, the 6-8 equations in system (1) are written as

$$\left\{ \begin{aligned} & \frac{d\vartheta_{ir}}{dt} - \frac{\vartheta_{i\varphi}^2}{r} = k_i (V_r - v_{ir}), \\ & \frac{d\vartheta_{iz}}{dt} = k_i (V_z - v_{iz}), \\ & \frac{d\vartheta_{i\varphi}}{dt} + \frac{\vartheta_{ir} \vartheta_{i\varphi}}{r} = k_i (V_\varphi - v_{i\varphi}). \end{aligned} \right. \tag{3}$$

In this system, the derivative in the right parts of the equations is the substantial derivative

$$\frac{d}{dt} = \frac{\partial}{\partial t} + \vartheta_{ir} \frac{\partial}{\partial r} + \vartheta_{iz} \frac{\partial}{\partial z}. \tag{4}$$

To search for particle trajectories, it is necessary to add the following equations to system (3)

$$\frac{dz_i}{dt} = \vartheta_{iz}, \quad \frac{dr_i}{dt} = \vartheta_{ir}. \tag{5}$$

For the numerical solution of system (1), a current function  $\psi$  is introduced, which satisfies the continuity condition for

$$V_r = -\frac{1}{r} \frac{\partial \psi}{\partial z}, \quad V_z = \frac{1}{r} \frac{\partial \psi}{\partial r}. \tag{6}$$

Vorticity  $\zeta$  is also introduced

$$\zeta = \frac{\partial V_z}{\partial r} - \frac{\partial V_r}{\partial z}. \quad (7)$$

In the second equation of system (1) the derivative with respect to  $r$  is taken and in the third equation - with respect to  $z$ . Subtracting the results, exclude the pressure and get the following system of equations for the air flow in new variables:

$$\frac{\partial \zeta}{\partial t} + V_r \frac{\partial \zeta}{\partial r} + V_z \frac{\partial \zeta}{\partial z} - \frac{V_r \zeta}{r} + 2V_\varphi \frac{\partial V_\varphi}{\partial z} = \frac{\partial}{\partial r} \left[ \frac{1}{r} \frac{\partial (r \tilde{v} \zeta)}{\partial r} \right] - \frac{\partial}{\partial r} \left[ \sum_{i=1}^N \frac{\rho_i}{\rho} k_i (V_z - v_{iz}) \right],$$

$$\frac{\partial}{\partial r} \left( \frac{1}{r} \frac{\partial \psi}{\partial r} \right) + \frac{\partial}{\partial z} \left( \frac{1}{r} \frac{\partial \psi}{\partial z} \right) = \zeta. \quad (8)$$

For numerical implementation of system (8) the computational domain is reduced to a rectangular one. To do this, perform the following coordinate transformation:

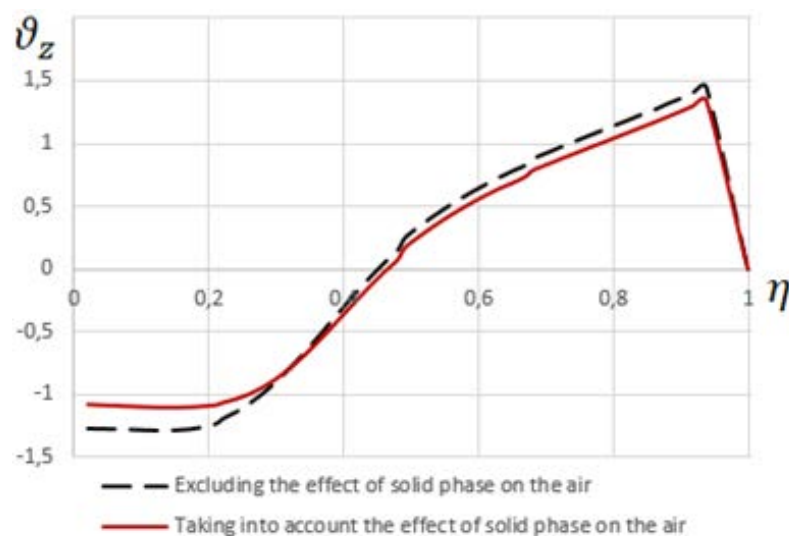
$$\xi = \frac{z}{L}, \quad \eta = \frac{r}{f(z)},$$

$$f(z) = \begin{cases} R_2 & \text{if } z < 0.2L \\ R_2 - \frac{R_2 - h}{L}z & \text{if } 0.2L < z < L. \end{cases}$$

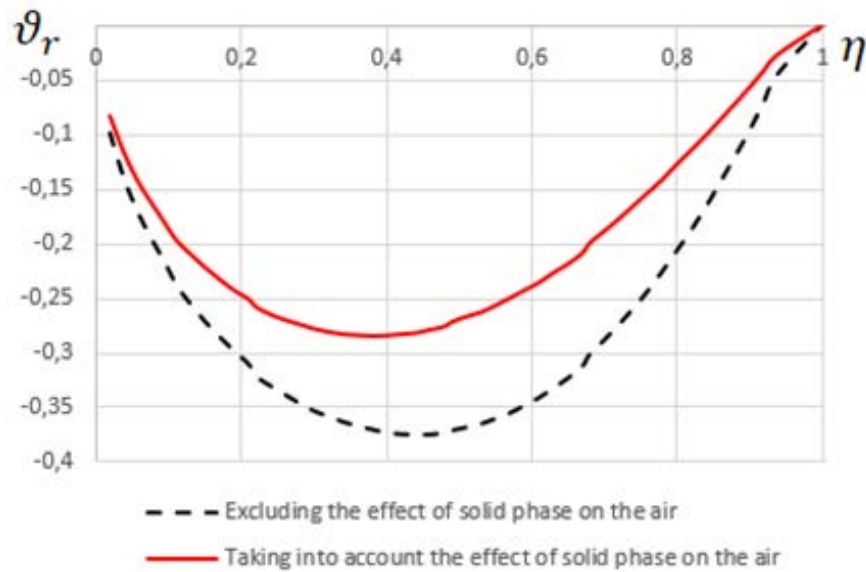
To ensure the stability of the computational process in approximating convective terms, the A.A. Samarsky [11] difference scheme against the flow is used, and the diffusion terms are approximated by a central difference. The Poisson equation for the flow function is also approximated by the central difference, and to solve it, the method of iteration of over-relaxation has been used.

To integrate the equations of motion of particles (2), the Euler method with recalculation has been used. Therefore, this system of equations is integrated with the second-order accuracy.

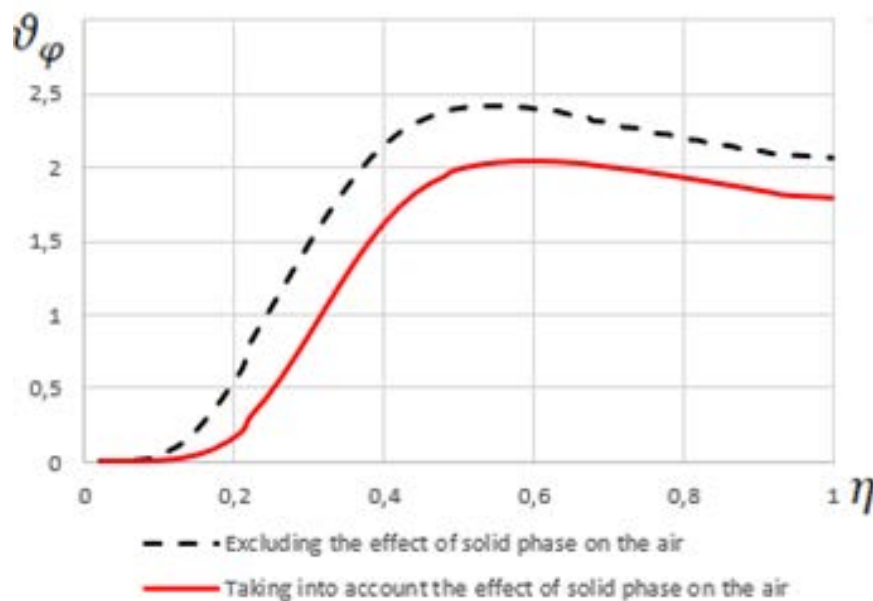
The parameters of laboratory device of the dust catcher have the following values:  $R_1 = 12 \text{ cm}$ ,  $R_2 = 20 \text{ cm}$ ,  $h = 8 \text{ cm}$ ,  $L = 300 \text{ cm}$ . The experiments have been conducted at the following values of the flow parameters at the inlet to coaxial channel:  $V_z = 4.1 \frac{\text{m}}{\text{sek}}$ ,  $V_r = 0$ ,  $V_\varphi = \frac{1.8 \text{ m}^2}{r \text{ sek}}$ ,  $\rho^0 = 7000 \frac{\text{kg}}{\text{m}^3}$ . The total density of the solid phase at the inlet is  $\sum_{i=1}^N \rho_i = 18 \text{ g/m}^3$  and it is uniformly distributed over the cross section. Figures 2-4 illustrate air velocity profiles in cross section  $\xi = 0.5$ . In these graphs, the dotted lines show the changes in the parameters not considering the effect of the solid phase on the air flow, and the solid lines - considering them.



**Figure 2.** Axial airflow velocity profiles in cross section  $\xi = 0.5$

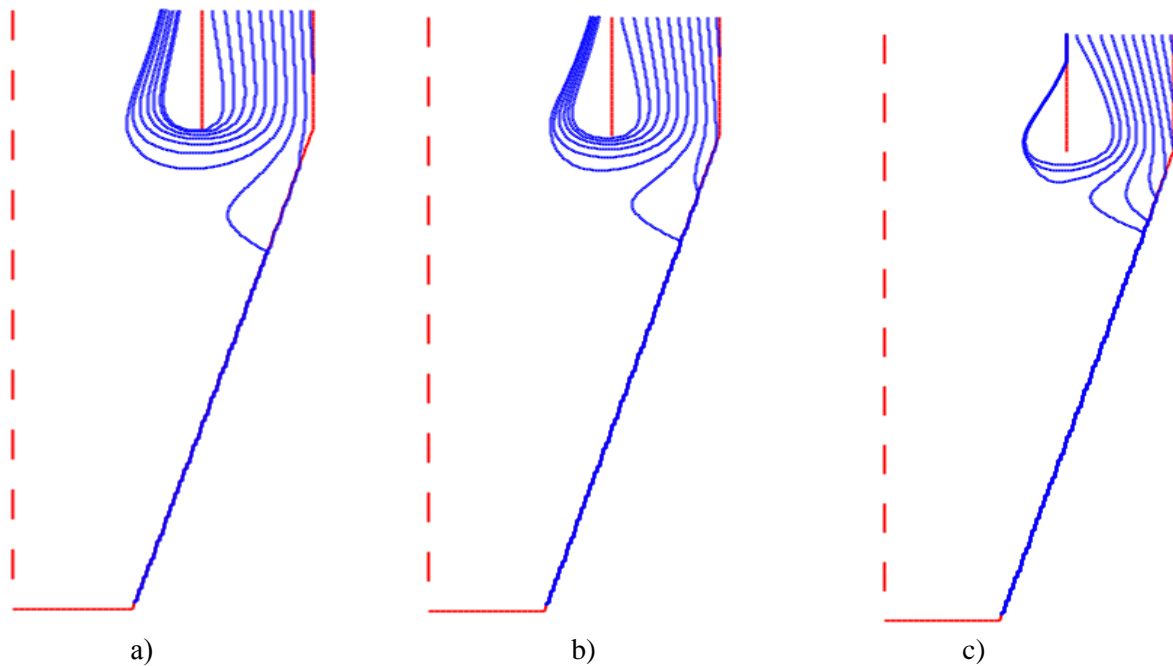


**Figure 3.** Radial airflow velocity profiles in cross section  $\xi = 0.5$



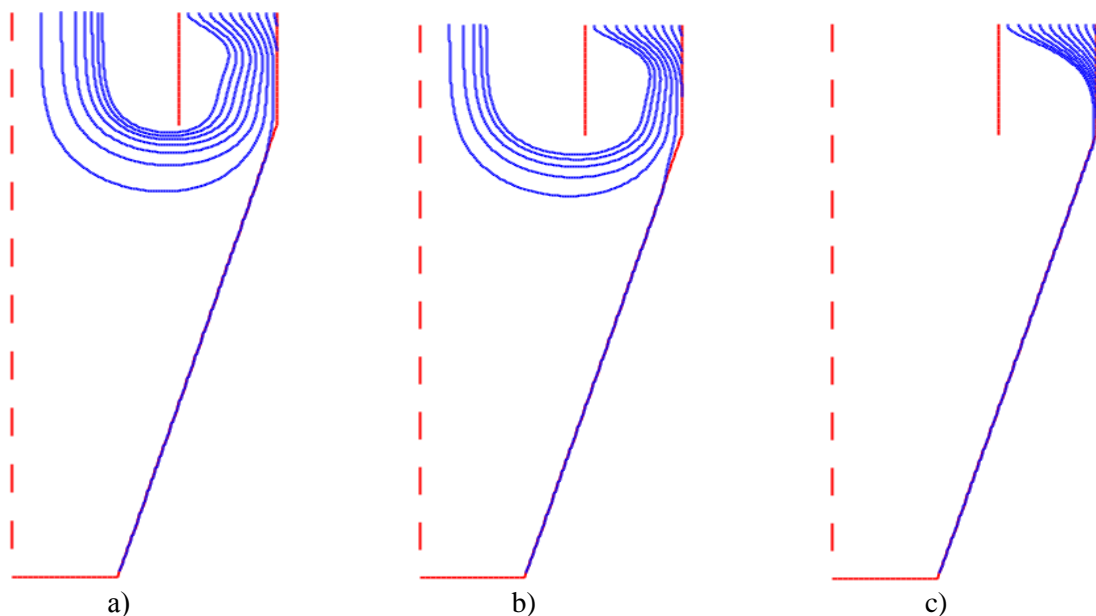
**Figure 4.** Tangential airflow velocity profiles in cross section  $\xi = 0.5$

Figure 5 shows the trajectories of dust particles of diameters  $\delta = 7 \text{ mkm}$ ,  $\delta = 10 \text{ mkm}$ ,  $\delta = 13 \text{ mkm}$ , obtained without consideration of the effect of the solid phase on the air flow. As seen from the figure, approximately 10% of particles of a diameter of  $\delta = 7 \text{ mkm}$  are “caught” by a dust catcher, i.e. falls into the bunker.



**Figure 5.** Particle trajectories without consideration of the effect of the solid phase on the air flow a)  $\delta = 7 \text{ mkm}$ , b)  $\delta = 10 \text{ mkm}$ , c)  $\delta = 13 \text{ mkm}$ .

Calculation of the efficiency of the dust catcher is of great interest. For this purpose, dust is fed to the inlet, the dispersed composition of which is shown in Fig. 6



**Figure 6.** Particle trajectories considering the effect of the solid phase on the dynamics of the air flow. a)  $\delta = 7 \text{ mkm}$ , b)  $\delta = 10 \text{ mkm}$ , c)  $\delta = 13 \text{ mkm}$ .

Disperse analysis of the powder has been performed with the “Malvern” laser analyzer. To compare the results of numerical calculation with the experimental data, a dispersion analysis of the

dust from the bag filter has been conducted, i.e. the dust not caught by centrifugal dust catcher. Figure 7 presents the dispersed composition of the zinc dust entering the dust catcher.

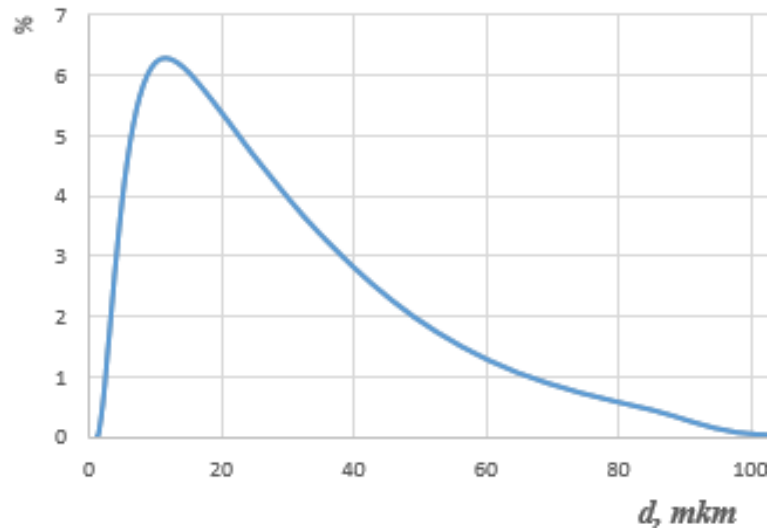


**Figure 7.** Dispersed analysis of the original zinc powder

Figure 7 presents the dispersed composition of dust from a bag filter by the analyzer (dots) and by numerical calculation using the model described above (solid line). As seen from this figure, the agreement of the calculated results with the data obtained from the analyzer is satisfactory.

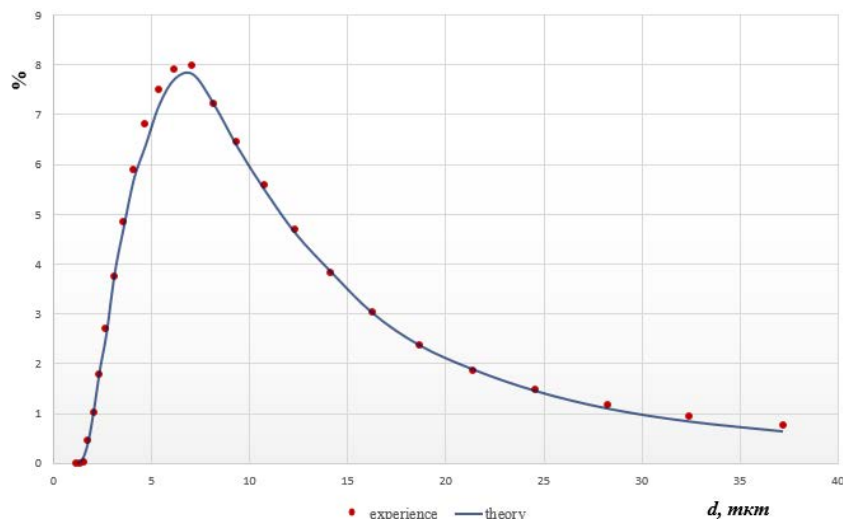


**Figure 8.** Disperse analysis of the dust composition from the bag filter

**Conclusion.** It is shown in the paper that the SARC turbulence model adequately describes a swirling flow inside the centrifugal devices, in particular in a dust catcher. Therefore, this model can be successfully used in the search of optimal parameters of centrifugal dust catchers and other devices with swirling flows.

## References

- [1] Spalart P R and Allmaras S R 1994 A one-equation turbulence model for aerodynamic flows 1 pp 5–21 AIAA Paper, 1992-0439.

- [2] Menter F R Zonal two-equation  $k-\omega$  turbulence models for aerodynamic flows// AIAA Paper, 1993-2906.
- [3] Spalart P R and Shur M L 1997 On the sensitization of turbulence models to rotation and curvature *Aerospace Science and Technology* Vol **1** 5 pp 297-302
- [4] Smirnov P and Menter F 2008 Sensitization of the SST turbulence model to rotation and curvature by applying the Spalart-Shur correction term // *Proc. of ASME Turbo Expo: Power for Land, Sea and Air, GT 2008 (Germany, Berlin, June 9-13, 2008)* 10
- [5] Vasilevsky M V and Zykov E G 2005 Calculation of gas cleaning efficiency in inertial devices (Tomsk: TPU publishing house) 86 p.
- [6] Shilyaev M I and Shilyaev A M 2003 Simulation of the dust collection process in a direct-flow cyclone. 1. Aerodynamics and the diffusion coefficient of particles in a cyclone chamber *Thermal Physics and Aeromechanics* V 10 2 pp 157–170
- [7] Shilyaev M I and Shilyaev A M 2003 Simulation of the dust collection process in a direct-flow cyclone. 2. Calculation of fractional leakage coefficient *Thermo physics and aeromechanics* Vol **10** 3 pp 427–437
- [8] Baranov D.A., Kutepov A.M., Lagutkin M.G. 1996 Calculation of separation processes in hydro-cyclones *Theoretical foundations of chemical technology* Vol **30** 2 pp 117–122.
- [9] Akhmetov T G, Porfileva RT and Gaisin L G 2002 Chemical technology of inorganic substances Book 1 (Moscow: Higher School) 688 p.
- [10] Nigmatulin R. I., Dynamics of multiphase media. Ch. I and II. M.: Nauka, 1987, p.464.
- [11] Samarsky A A 1977 *Theory of difference schemes* (Moscow: Publishing House "Nauka")